Simulation and design of a one-sided distributed optical sensor for wafer tracking

J.F. Elfferich (4565339), F.J. van Melis (4590384),
T. Neeft (4558480) and A.P. Tiktak (4585992)
Group: PME-A7-2019

***Abstract*— This paper presents a working prototype of a two-dimensional, one-sided, distributed optical sensor using an array of glass fibers. This concept is designed to track thin Si-substrates such as Si-wafers or solar cells on actuated air film transportation systems. Simulations were used to determine the relation between the grid pattern and the accuracy, and the precision of the system. Using a low density square grid of 2500 fibers/m^2 and a substrate with a diameter of 64.5 mm, an accuracy of 0.026 mm, average error of 0.173 mm, and precision (standard deviation) of 0.094 mm were obtained in the simulated situation along a straight path. The actual prototype reached an accuracy of 0.127 mm, an average error of 0.592 mm, and a precision of 0.803 mm under the same circumstances.**

I. Introduction

Current wafer handling includes complex robot arms that physically grab and place wafers in processing stations. Unfortunately, this makes wafers susceptible to breaking. The negative impact this has on cost effectiveness is of growing concern, since the risk of breaking is increasing as substrates are manufactured larger and thinner. Already, the dominating front-end costs of wafer manufacturing, include a substantial amount of wafers having defects, according to Flamm [1]. There has been research into the optimal way to alter the properties of the wafer itself to make it less prone to breaking [2], but recent research into new ways of handling the substrate with more care seems like a viable next step. Previous works into actively steering any substrate using an air film seems promising [3], [4], as this method does not impose as much stress as conventional handling, and possibly reduces surface contamination [5].

The proposed concept expands the knowledge and applicability of air film handling by adding an accurate two-dimensional position sensor using a grid of glass fibers. Conventional position sensors cannot always conveniently be used in combination with air film handling since these sensors often require more space than available. E.g. in an industrial setting it would be desired to leave the area above the surface unoccupied to accommodate for manufacturing equipment. Using sensors attached along the sides is impractical, since the substrates are very thin (less than 1 mm) which makes them hard to track. The developed concept uses the space below the surface sparingly; only small holes in which a glass fiber protrudes are present in the plane. This allows for future integration of this sensor concept in an air bearing system.

Contact information:
J.F.Elfferich@student.tudelft.nl,
F.J.vanMelis@student.tudelft.nl,
T.Neeft@student.tudelft.nl and
A.P.Tiktak@student.tudelft.nl

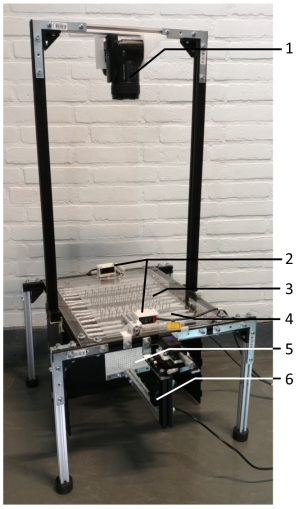

Fig. 1. The prototype; 1: Overhead Casio camera. 2: Laser distance sensors. 3: Glass fibers in acrylic plate. 4: LED strip. 5: Receiving plate glass fibers. 6: USB camera.

Ultimately, the aim of this project is to develop and build a prototype of a one-sided distributed optical sensor, using glass fibers, to dynamically track a substrate moving along a plane. The goal is to show proof of concept and achieve an accuracy below 1 mm and a precision (defined as standard deviation) below 0.5 mm, using a low density grid. It is also required to design the system to have equal performance in two dimensions. Due to time and monetary constraints no air bearing system was integrated into the position sensor prototype.

In order to reach these goals, the relation between the pattern and density of the grid in which the mentioned glass fibers are placed, and the achievable accuracy and precision, is determined through simulations. As there was little relevant data found in papers, a MATLAB script was developed to create or import grids and subsequently subject them to simulations across different paths to establish their effectiveness. In addition, software that can simulate, collect data and predict the performance of the sensor has been created and tested.

This paper will start with the theory used for the locating the wafer's position, which is followed by an explanation of the prototype and methods used. The results and discussions show and debate the outcomes after which the conclusions and recommendations present some final thoughts.

This entire design study has been conducted as part of the Bachelor End Project for Mechanical Engineering students at the TU Delft in the third year of their Bachelor studies.

II. Theory

This section will shortly explain the theory used to predict the location of the wafer using the data of the glass fibers as an input. Using realistic assumptions, least squares equations can be formulated and solved for the position, given a set radius. These equations are based on the work of Chernov and Lesort [6] and Gander, Golub and Strebel [7]. They fit circles with some optimal radius through given points. Their work has been adapted into the following theory.

A. Assumptions

It is assumed that the wafer is moving with a stable acceleration, as the friction coefficient between the wafer and surface is expected to be constant.

B. Mid-point error

Using the above assumption, a good prediction of the position of a moving wafer can be made, even if the wafer does not cover new fibers on a given instance. Given the accurate prediction of the mid-point of the wafer, the following least squares equation can be formulated:

$$(x_i - x_c - \epsilon_x)^2 + (y_i - y_c - \epsilon_y)^2 = R^2 \tag{1}$$

Here x_i and y_i are the coordinates of a detected point on the edge of the wafer. x_c and y_c are the coordinates of the mid-point that is predicted using the last known speed, acceleration and position of the wafer. ϵ_x and ϵ_y are the errors of the predicted midpoint with respect to the actual mid-point. R is the radius of the wafer.

This equation results in the following optimization problem:

$$\sum_{i=1}^{n} \left(x_{i*}^2 + y_{i*}^2 - 2x_{i*}\epsilon_x - 2y_{i*}\epsilon_y + \epsilon_x^2 + \epsilon_y^2 - R^2\right)^2 \tag{2}$$

In this equation, $x_i - x_c = x_{i*}$ and $y_i - y_c = y_{i*}$ and n is the amount of edge-points used in the calculation.

Now, when assuming the prediction is sufficiently accurate, ϵ^2-terms can be neglected and the equation becomes:

$$\sum_{i=1}^{n} \left(x_{i*}^2 + y_{i*}^2 - 2x_{i*}\epsilon_x - 2y_{i*}\epsilon_y - R^2\right)^2 \tag{3}$$

Differentiating equation 3 to x and y results in the following system of equations:

$$\begin{bmatrix} \sum (x_{i*}^2) & \sum (x_{i*}y_{i*}) \\ \sum (x_{i*}y_{i*}) & \sum (y_{i*}^2) \end{bmatrix} \begin{bmatrix} \epsilon_x \\ \epsilon_y \end{bmatrix} = \begin{bmatrix} \sum (x_{i*}^3) + \sum (x_{i*}y_{i*}^2) - \sum (x_{i*})\, R^2 \\ \sum (x_{i*}^2 y_{i*}) + \sum (y_{i*}^3) - \sum (y_{i*})\, R^2 \end{bmatrix}$$

Solving this system of equation gives values for ϵ_x and ϵ_y. The corrected coordinates of the mid-point are determined by adding the error to the predicted mid-point.

$$x_{new} = x_c + \epsilon_x \quad y_{new} = y_c + \epsilon_y \tag{4}$$

C. Simulation

In order to simulate the movement and detection of the wafer, a model was made using MATLAB, see Fig. 2 for the flow diagram. The model works by creating a path over a grid containing the positions of the glass fibers (sensors). When the output from a sensor changes from *off* to *on* or from *on* to *off*, the coordinates of that sensor are saved. The last five or six saved coordinates are used as an input for the mid-point error calculation. Every time step, these saved sensor locations are moved along with the predicted mid-point using the current speed of the wafer. This way, the location of the wafer can be estimated even if there is no new input. Also, every time a new point is detected, this point can be assumed to be exactly on the edge of the wafer while the older points could contain an error due to a small deviation in the calculated speed. In order to use this information to make the calculation more precise, the new point is to be given a larger weight factor.

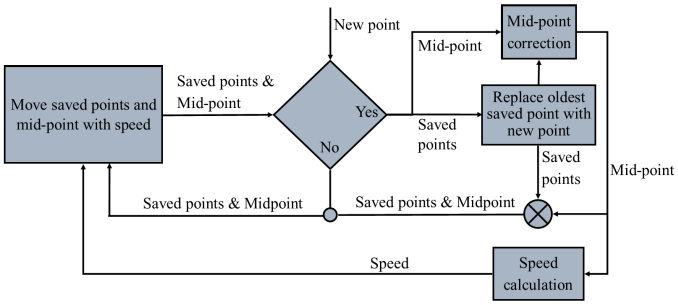

Fig. 2. Flow diagram of the simulation model

III. Methods

In this section the overall design of the prototype is outlined. The position determined using the distributed sensor is compared with the results obtained using a reference camera and a laser-interferometer. Furthermore, the image recognition script that decodes the USB camera input into a matrix is explained.

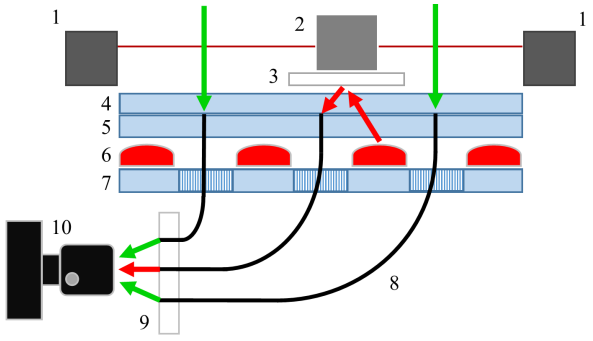

Fig. 3. Schematic view of the proposed concept, the red light can be seen reflected (red arrows). The green arrows indicate surrounding (polluting) light. 1. Laser-interferometers 2. PVC tube 3. Teflon wafer substrate 4. Top plate 5. Plate holding fibers 6. LED strip 7. Bottom plate for LED strips 8. Glass fibers 9. Receiving plate glass fibers 10. USB camera

A. The design of the prototype

To test the designed glass fiber sensor, a rigid, adjustable frame was produced, see Fig. 1. The size of the upper surface is 480x380 mm, to ensure enough space for the sensors and the wafer to travel on. The legs holding the surface are 300

mm long to allow for sufficient clearance for the glass fibers to be connected between the table's surface and the webcam's reception plate. The webcam has a clear view of the ends of the glass fibers embedded in the reception plate, see Fig. 3. For reference position data, a high fps Casio camera, overlooking the surface from above, was used to track the wafer with image recognition script. As a second reference system, two laser distance sensors were used. By aligning them on the PVC tube, the location of the wafer could be calculated conveniently using a MATLAB script and the outputted data.

B. Image recognition

To gather the information from the glass fibers, image processing has been used on the data captured with the USB webcam. The software (based on *Image Analyst's* [8]) can define the boundaries of all fibers. To process the information of the video, the intensity of each glass fiber within the mentioned boundary is calculated for every frame of footage. An example of the determined boundaries and the intensity is shown in Fig. 4.

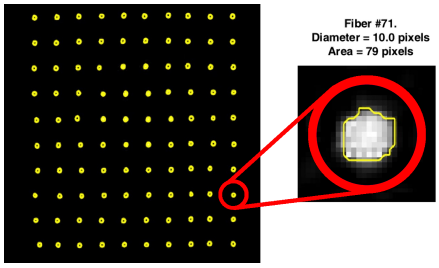

Fig. 4. Left: the boundaries of all the glass fibers determined by image processing, right: magnification of a single fiber with a yellow boundary.

The overhead Casio camera also uses image processing. In this case, a custom script based on Bose's [9] is used to locate a LED in the middle of the wafer. The software first removes the perspective at the level of the LED. Simultaneously, the size of each pixel is mapped. After this calibration step, the known diameter of the wafer along with the clearly visible, white LED is used to calculate the location of the wafer.

IV. Results

As mentioned in section I, the pattern in which the glass fibers are placed was considered to be one of the key factors in the accuracy the system could achieve. To test this, 20 simulations for each grid were performed with some of the results set out in Table I. For readability and as a reference to the actual prototype, the fiber density was set to 100 fibers for this table, on a 200 by 200 mm grid (what amounts to 2500 fibers/m^2) with a substrate of 64.5 mm. Imitating a substrate, a circle was simulated along a path that triggered the underlying fibers. Three different paths were compared; a straight line, a curve and a circular path. To ensure the path was not beneficially placed for a certain grid, the circle travelled along the path 20 times, each time with a different starting point.

The most accurate grids are set out in the rows of Table I, some grids were designed with a pattern, others were created randomly using MATLAB. The hundreds of

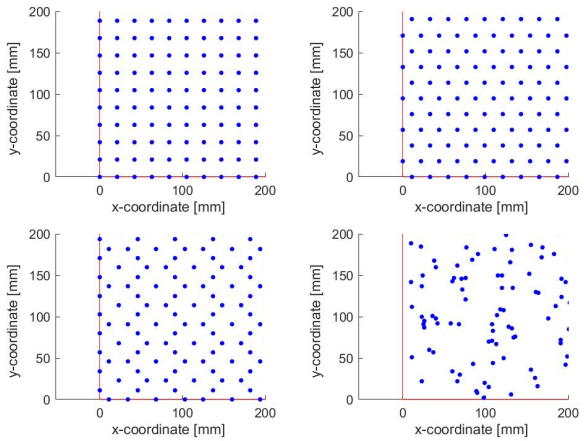

Fig. 5. Four examples of the tested grids. Top left: square_v1; top right: triangle; bottom left: custom_v9; bottom right: an example random grid.

randomly created grids were tested to determine their average error and variance. Only grids with an average error below a threshold of 0.4 mm were saved. Out of this test rose the observation that the most successful grids had a somewhat uniform fiber distribution, see Fig. 5.

A simulated accuracy of 0.026 mm is achieved when traveling along a straight line across a square grid with 2500 fibers/m^2 using a substrate with a diameter of 64.5 mm. Table I also shows an average error of 0.173 mm and a precision (standard deviation) of 0.094 mm. The actual prototype reached an accuracy of 0.127 mm, a precision of 0.803 mm and an average error 0.592 mm, see also section V.

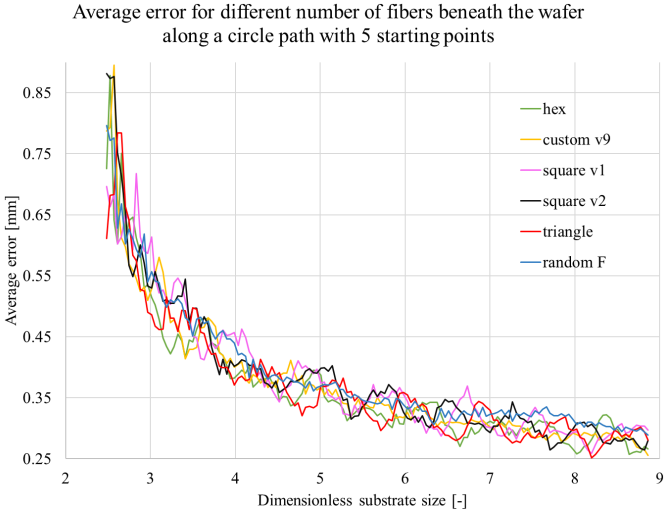

Fig. 6. Graph containing the average error of the six most accurate grids, evaluated along the dimensionless substrate size. The standard deviation is left out for readability.

Along a more general curved path, the simulation achieved an accuracy of 0.128 mm, a standard deviation of 0.397 mm and an average error of 0.445 mm.

To investigate the relationship between the size and type of grid and the performance of the system, Fig. 6 was created amongst others. The dimensionless substrate size is set along the x-axis of this graph. This corresponds with taking the

TABLE I

AVERAGE ERROR AND ACCOMPANYING VARIANCE, IN MM, OF A SIMULATED 64.5 MM WAFER ON DIFFERENT GRIDS ALONG 3 DIFFERENT PATHS WITH 20 DIFFERENT STARTING POINTS, WITH A FIBER DENSITY OF 2500 FIBERS/M^2

grid name	line	variance	curve	variance	circle	variance
hex	0.144	0.006	0.412	0.155	0.341	0.097
custom_v4	0.164	0.009	0.553	0.231	0.744	1.646
custom_v6	0.182	0.013	0.728	0.587	0.616	1.219
custom_v7	0.173	0.010	0.605	0.389	0.507	0.280
custom_v9	0.140	0.006	0.410	0.144	0.333	0.074
square_v1	0.173	0.009	0.446	0.158	0.375	0.085
square_v2	0.132	0.006	0.426	0.151	0.333	0.078
square_v3	0.143	0.006	0.570	0.414	0.420	0.145
triangle	0.143	0.006	0.376	0.133	0.325	0.073
random_a	0.174	0.009	0.446	0.158	0.375	0.085
random_b	0.164	0.009	0.424	0.122	0.564	0.537
random_c	0.165	0.016	0.515	0.270	0.376	0.089

square root of the area of the wafer multiplied with the fiber density.

The graph shows a decrease in the average error of the location prediction the system makes, when evaluated with an increased substrate size. Fig. 6 also shows that not a single grid has the lowest average error across all substrate sizes.

V. DISCUSSION

As mentioned in section IV, results from the experiments differ from those of the simulations, achieving an average error of 0.592 mm compared to 0.173 mm in simulation. Probable causes are fluctuations in the substrate's velocity during experiments. This reduces the performance, since the algorithm is optimized to work with constant acceleration. Additionally, increased noise due to ambient light and fabrication inconsistencies negatively impacted performance, despite fiber calibration.

Based on Fig. 6, it seems likely that there is a limit to the minimal average error that can be achieved by increasing fiber density and/or substrate size: about 0.25 mm for this configuration. This limit probably originates from the optimization steps taken when designing the software. Specific constants and formulae were used that work optimally with a relatively sparse input. For a more general case, a custom script with a Kalman filter was produced during the project, which proved to track the wafer accurately if the noise was precisely known. During the project this script was not used for data collection as the noise was not determined precisely enough to succeed the precision of the already mentioned method, see section II-C.

Furthermore, the error seems to have local minimums at regular intervals (see Fig. 6). A possible explanation for this phenomenon would be that certain combinations in geometry of the substrate and grid can cause a specifically good combination of edge detection points. The significantly lower fluctuations in average error of the random grid also fits within this theory.

VI. CONCLUSIONS AND RECOMMENDATIONS

It proved to be possible to demonstrate a one-sided, two-dimensional distributed optical positions sensor using glass fibers, although not as accurate as the simulations predicted. The prototype was able to track a circular substrate with ample precision and accuracy, see section IV. Systems using linear sensor arrays with photosensitive diodes are competitive in this field, since they are able to achieve sub-millimeter accuracy, although these require a higher density of sensors to do so [10]. However, with further improvements in fiber density, track length and data handling, the prototype's concept could offer superior performance as a precise location sensor in a real time transportation system. Additionally, mentioned grids could also be tested in a new prototype to further explore the relation between the dimensionless substrate size and the average error, as depicted in Fig. 6.

Further research can also be done to investigate the optimal grid for other shapes of substrates, or for a specific required path. As human creativity reaches its limits, machine learning might be used to create and evaluate grids more efficiently.

Finally, it will likely prove to be challenging to fully integrate the sensor system with an air bearing system, such as Vagher's [11], without impacting the system's performance. For example, the light sources may be obstructed, in which case installing duplex glass fibers for supplying light in parallel could be a viable solution.

Although enough challenges remain, the developed prototype shows proof of concept, and the simulations give tremendous insight into the main design parameters, so an actual air film system with positional feedback seems one step closer.

ACKNOWLEDGEMENTS

We would like to thank our two supervisors; Dr.ir. J.F.L. Goosen and Dr.ir. R.A.J. van Ostayen. They supported our project tremendously with weekly meetings and helpful tips and recommendations throughout the entire project.

REFERENCES

[1] K. Flamm, "Moores law and the economics of semiconductor price trends," *International Journal of Technology, Policy and Management*, vol. 3, no. 2, p. 127, 2003.

[2] X. F. Brun and S. N. Melkote, "Analysis of stresses and breakage of crystalline silicon wafers during handling and transport," *Solar Energy Materials and Solar Cells*, vol. 93, no. 8, p. 12381247, 2009.

[3] J. Wesselingh, "Contactless positioning using an active air film," Ph.D. dissertation, Delft University of Technology, 2011.

[4] J. Snieder, "Development of an air-based contactless transport demonstrator," Master's thesis, Delft University of Technology, Oct 2017.

[5] J. V. Rij, J. Wesselingh, R. V. Ostayen, J. Spronck, R. M. Schmidt, and J. V. Eijk, "Planar wafer transport and positioning on an air film using a viscous traction principle," *Tribology International*, vol. 42, no. 11-12, p. 15421549, 2009.

[6] N. Chernov and C. Lesort, "Least squares fitting of circles and lines," Feb 2008.

[7] W. Gander, G. Golub, and R. Strebel, "Least-squares fitting of circles and ellipses," 1995.

[8] ImageAnalyst, *Image Segmentation Tutorial*, 2015. [Online]. Available: https://nl.mathworks.com/matlabcentral/fileexchange/25157-image-segmentation-tutorial

[9] A. Bose, *How to Detect and Track Red, Green and Blue Colored Object in LIVE Video*, 2016. [Online]. Available: https://nl.mathworks.com/matlabcentral/fileexchange/40154

[10] Y. Voorrips, "Distributed sensing for contactless substrate transport," Master's thesis, Delft University of Technology, Aug 2017.

[11] E. P. Vagher, "Contactless passive transport of thin solar cells," Master's thesis, Delft University of Technology, Oct 2016.